Electronic band parameters for zinc-blende $Al_{1-x}Ga_xN$

2002 J. Phys.: Condens. Matter 14 7017

(http://iopscience.iop.org/0953-8984/14/29/303)

INSTITUTE OF PHYSICS PUBLISHING JOURNAL OF PHYSICS: CONDENSED MATTER

J. Phys.: Condens. Matter **14** (2002) 7017–7026 PII: S0953-8984(02)33493-3

Electronic band parameters for zinc-blende $Al_{1-x}Ga_xN$

A Bhouri, F Ben Zid, H Mejri, A Ben Fredj, N Bouarissa[1] and M Said

Unité de Physique des Solides, Département de Physique, Faculté des Sciences de Monastir, 5019 Monastir, Tunisia

E-mail: moncef.said@fsm.rnu.tn

Received 6 February 2002, in final form 29 May 2002
Published 11 July 2002
Online at stacks.iop.org/JPhysCM/14/7017

Abstract

Band-structure calculations are performed for cubic $Al_{1-x}Ga_xN$ using the empirical pseudopotential method. The band gaps at Γ, X and L points and the electron effective masses of Γ and X valleys are calculated as a function of the gallium fraction x. It is found that there is no significant change in these electronic band parameters on taking into account the alloy disorder. On the basis of a model solid theory, we have calculated the band discontinuities for heterointerfaces between strained $Al_{1-x}Ga_xN$ and relaxed $Al_{1-y}Ga_yN$. The latter calculations are extended to the whole range of compositions x and y. The information derived from this investigation will be useful in the design of lattice-mismatched heterostructures in blue-light optoelectronics applications.

1. Introduction

III–V nitrides have been extensively investigated in recent years because of their scientific and technological interest (for a review see [1–3]). In particular, the $Al_{1-x}Ga_xN$ alloy system covers a wide ultraviolet (UV) spectral range between the band gap of 3.4 eV for GaN and 6.2 eV for AlN at room temperature, and is very attractive for short-wavelength optical applications such as in UV light emitters and UV detectors [4]. In addition, $Al_{1-x}Ga_xN$ is used to form strained heterostructures with GaN and $In_xGa_{1-x}N$ in light-emitting diodes and in $GaN/Al_{1-x}Ga_xN$ field-effect transistors [4].

Until the middle of the last decade, GaN in the hexagonal wurtzite phase was the only known polytype [5]. More recently, with the progress in epitaxy growth, GaN of zinc-blende type has been grown successfully [5]. According to the general trends of the material properties of III–V compound semiconductors, zinc-blende GaN should be better suited for controlled n- and p-type doping than wurtzite. This latter system usually exhibits a high n-type background carrier concentration, mostly originating from native defects and/or from residual

[1] Present address: Physics Department, University of M'sila, 28000 M'sila, Algeria.

impurities [5]. Moreover, cubic GaN has a higher drift velocity and a somewhat lower band gap than the wurtzite structure [6]. AlN can be grown in both wurtzite and zinc-blende forms as well [6]. The existence of GaN and AlN in two crystal phases with different electron band structures adds further interest to the $Al_{1-x}Ga_xN$ alloy system.

Direct and indirect energy gaps, electron and hole effective masses as well as their composition dependences are the most critical parameters for band-structure calculations of III–V nitride alloys. Therefore, an accurate knowledge of these parameters for $Al_{1-x}Ga_xN$ is very important. Moreover, calculation of band offsets for cubic $Al_{1-x}Ga_xN$ is useful for calculating the energy bands in quantum heterostructures. Unfortunately, there appears to be limited experimental and theoretical information in the literature at present, regarding the electronic band parameters for zinc-blende $Al_{1-x}Ga_xN$ ternary alloys [3]. This has inspired us to carry out such a calculation of the electronic band parameters for zinc-blende $Al_{1-x}Ga_xN$. For this purpose, we have used the empirical pseudopotential method (EPM) under the virtual crystal approximation (VCA), both disregarding and taking into account the effect of alloy disorder. Calculations of band offsets have been performed on the basis of a model solid theory [7] which has two main aspects. The first is the generation of an accurate band structure by performing density-functional calculations on individual bulk semiconductors. The second is the establishing of a reference level that can be used for a line-up procedure. This reference, denoted as $E_{v,av}$, is defined as the average over the three uppermost valence bands at the Γ point of the Brillouin zone. This permits us to evaluate the energy levels on an absolute energy scale, and allows us to derive band line-ups by simply subtracting values for individual semiconductors.

The paper is organized as follows: after a brief introduction, we report in section 2 results on the band-gap energy, the electron effective masses and the band offsets calculated for $Al_{1-x}Ga_xN$ as a function of the molar fraction x; our conclusions are summarized in section 3.

2. Results and discussion

2.1. Band-gap energy

The band-structure calculation is based on the EPM in which the pseudopotential form factors are fitted to experiment using a non-linear squaring procedure [8]. In the case of zinc-blende semiconductor compounds, six pseudopotential form factors and a set of 59 plane waves are sufficient for calculating the band structure. The compositional disorder is taken into account by adding a non-periodic potential to the VCA [9]. This method will be called the 'improved VCA'. For the cubic $Al_{1-x}Ga_xN$ being studied here, the symmetric and antisymmetric form factors are expressed as [9, 10]

$$V^{S,A}_{\mathrm{AlGaN}}(G) = (1-x)V^{S,A}_{\mathrm{AlN}} + xV^{S,A}_{\mathrm{GaN}} + p[x(1-x)]^{1/2}(V^{S,A}_{\mathrm{AlN}} - V^{S,A}_{\mathrm{GaN}}) \tag{1}$$

where p is a parameter which simulates the disorder effect. It is treated as an adjustable parameter and has a value of zero when the compositional disorder is not included. As for the lattice constant of this ternary alloy, it is obtained according to Vegard's law:

$$a_{\mathrm{AlGaN}} = (1-x)a_{\mathrm{AlN}} + xa_{\mathrm{GaN}}. \tag{2}$$

In table 1, we give the adjusted pseudopotential form factors as well as the lattice constants for GaN and AlN [11]. The calculated band-gap energies for these materials along with the available data in the literature [3, 12, 13] are listed in table 2. The computed band-gap energies E_g^{Γ}, E_g^{X} and E_g^{L} as a function of composition x for zinc-blende $Al_{1-x}Ga_xN$ are plotted in figure 1. As can be seen, the direct band-gap energy at the Γ point and the indirect one E_g^{L} decrease with increased gallium content, whereas, the indirect band gap E_g^{X} decreases and

Table 1. Pseudopotential form factors and lattice constants for zinc-blende GaN and AlN.

Material	$V^S(3)$ (Ryd)	$V^S(8)$ (Ryd)	$V^S(11)$ (Ryd)	$V^A(3)$ (Ryd)	$V^A(4)$ (Ryd)	$V^A(11)$ (Ryd)	a (Å)
GaN	−0.502 636	−0.021 065	0.223 682	−0.032 595	0.200	0.135 464	4.5 [11]
AlN	−0.309 603	0.112 783	0.067 538	0.28	0.33	0.015	4.37 [11]

Table 2. Band-gap energies at Γ, X and L of GaN and AlN.

Material	E_g^Γ (eV)	E_g^X (eV)	E_g^L (eV)
GaN	3.2[a]; 3.299[b]	4.7[a]; 4.52[b]	6.2[a]; 5.59[b]
	3.38[c]; 3.24[d]	4.57[c]; 4.57[d]	5.64[c]; 6.04[d]
AlN	6.0[a]; 4.9[b]	4.9[a]; 6.0[b]	9.3[a]; 9.3[b]
	5.94[c]; 6.0[d]	5.10[c]; 4.9[d]	9.42[c]; 9.15[d]

[a] Present work.
[b] Reference [3].
[c] Reference [12].
[d] Reference [13].

then increases slightly with x. Hence, a crossover from an indirect to a direct band gap is found to be occurring at $x = 0.43$ and 0.47 corresponding to the band-gap energies of 4.4 and 4.4 eV using the VCA and improved VCA, respectively. This transition is induced by the Γ conduction band. The results obtained for E_g^Γ, E_g^X and E_g^L were fitted using a least-squares procedure. The analytical expressions are as follows:

$$\begin{aligned} E_g^\Gamma(x) &= 6.07 - 4.54x + 1.60x^2 \\ E_g^X(x) &= 4.91 - 1.86x + 1.62x^2 \qquad \text{(without disorder)} \\ E_g^L(x) &= 9.43 - 5.66x + 2.32x^2 \end{aligned} \tag{3a}$$

and

$$\begin{aligned} E_g^\Gamma(x) &= 6.09 - 3.98x + 1.00x^2 \\ E_g^X(x) &= 4.94 - 1.76x + 1.46x^2 \qquad \text{(with disorder)} \\ E_g^L(x) &= 9.41 - 4.70x + 1.39x^2. \end{aligned} \tag{3b}$$

All energies are in electron volts, the value of the adjustable disorder parameter p is 0.077 and the quadratic terms stand for the bowing parameter.

Initial studies of the compositional dependence of the band-gap energy reported downward, upward and negligible bowing [3]. Brunner *et al* [14] reported a bowing factor of 1.3 eV and the data of Huang and Harris [15] imply an even larger bowing parameter for $Al_{1-x}Ga_xN$ epilayers grown by pulsed laser deposition. Our results agree reasonably well with these two references when the VCA alone is used. Furthermore, they are in good agreement with the bowing parameter of 1.5 eV suggested by the cathodoluminescence measurements for $Al_{1-x}Ga_xN$ grown epitaxially on Si(111). However, the results of Albanesi *et al* [6] reported a weak upward bowing which has a value of −0.41 eV (see figure 1, symbols). Using the EPM under the VCA alone (without taking into account the compositional disorder), Fan *et al* [12] have also reported a weak but downward bowing of 0.05 eV. The results of [12] differ from ours. The discrepancy between our results and those of Fan *et al* lies in the fact that we have adjusted the pseudopotential form factors from the fit of different band-gap energies. Recently, Vurgaftman *et al* [3] in their review article have recommended continued use of the accepted bowing parameter of 1.0 eV. In order to introduce the compositional disorder effect into the

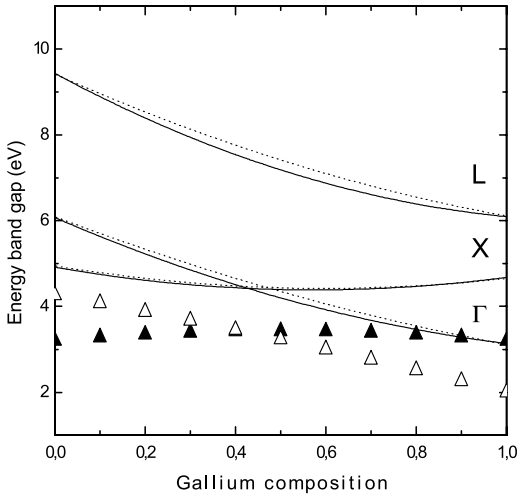

Figure 1. The x-dependent band gaps at the Γ, X and L points in zinc-blende $Al_{1-x}Ga_xN$ calculated without and with compositional disorder (solid/dotted curves). For comparison, also reported are LMTO band-gap results at Γ (empty triangles) and X (full triangles) taken from [6].

VCA, we have adjusted the disorder parameter p to obtain the bowing parameter of 1.0 eV. This value is achieved for $p = 0.077$ (equation (1)). On the other hand, our results regarding the crossing point are found to be in good agreement with those reported in the literature and which are for the composition range $x \approx 0.4$–0.6 [3]. Our crossing point value corresponds to a direct gap of 4.4 eV. This value is in disagreement with that of 3.22 eV reported by Albanesi *et al* [6]. It should be noted that our result is better than that of [6] since we have used an empirical method which starts from the fit of parent compounds to experiment, whereas in [6] the authors used the LDA which underestimates the band gaps. We point out that the compositional disorder slightly affects the principal energy band gaps (see figure 1, dotted curves). It is worth noticing that this effect is less important than that reported for $Ga_{1-x}In_xN$ [16]. This is due presumably to the lattice mismatch, which is more important in $Ga_{1-x}In_xN$.

2.2. Derivation of the electron effective masses

The effective mass is a necessary parameter for analysing the electron transport in bulk $Al_{1-x}Ga_xN$. It will be useful for the investigation of $Al_{1-x}Ga_xN$ quantum well structures as well. We adopt a parabolic line fit to the conduction band dispersion in the vicinity of the minima. The effective masses were calculated for the two lowest conduction bands Γ and X from the second derivative of the band energy with respect to the wavevector k. Figure 2 shows the electron effective mass at Γ (plot (a)) and X (plot (b)) calculated as a function of the gallium composition for zinc-blende $Al_{1-x}Ga_xN$ without and with disorder. As can be noted, the electron effective mass at Γ decreases on going from AlN to GaN, whereas the one at the X symmetry point shows a reverse trend as x increases. The best fit of the calculated electron effective masses has the form

$$\begin{aligned} m_{e,\Gamma}(x) &= 0.212 - 0.126x + 0.040x^2 \\ m_{e,\mathrm{X}}(x) &= 0.112 - 0.003x + 0.027x^2 \qquad \text{(without disorder)} \end{aligned} \tag{4a}$$

$$\begin{aligned} m_{e,\Gamma}(x) &= 0.212 - 0.108x + 0.020x^2 \\ m_{e,\mathrm{X}}(x) &= 0.112 - 0.005x + 0.028x^2 \qquad \text{(with disorder).} \end{aligned} \tag{4b}$$

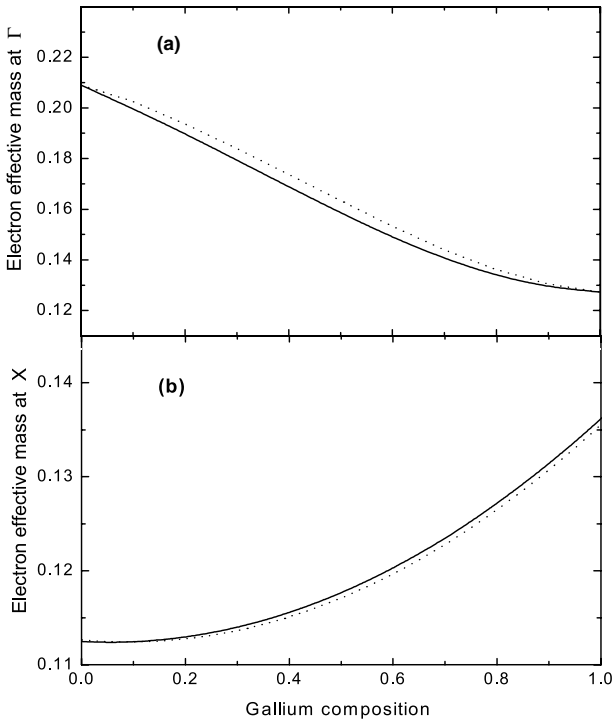

Figure 2. Electron effective masses of Γ (a) and X (b) valleys in cubic $Al_{1-x}Ga_xN$ as a function of composition x. The solid and dotted curves correspond to calculations without and with alloy disorder respectively.

All the effective masses are expressed in units of the free electron mass m_0. It is of particular interest that the compositional disorder does not significantly affect the electron effective mass at either Γ or X points. Once again, the effect of alloying disorder on the electronic mass parameters of zinc-blende $Al_{1-x}Ga_xN$ is weaker compared to that for cubic $Ga_{1-x}In_xN$ [16]. For the compounds GaN and AlN in the zinc-blende structure, table 3 shows the electron effective mass at the Γ symmetry point calculated in the present work. In the table also shown are other theoretical estimates [3, 12, 17, 18] and available experimental data [19] for comparison. As can be seen, the electron effective mass at the lowest conduction band for GaN obtained from our EPM calculations is smaller than the experimental value given in [19], but closer to the results reported in the works [12, 17]. In the case of AlN, there is no report of experimental data for the conduction band mass. Our EPM result for the electron effective mass at Γ of this binary agrees well with those reported by Fan *et al* [12] and Meney *et al* [18], but differs from the results calculated by Pugh *et al* [17] and Vurgaftman *et al* [3]. For the zinc-blende $Al_{1-x}Ga_xN$ investigated, we have calculated, on the other hand, the k-dependence of both $m_{e,\Gamma}(x)$ and $m_{e,X}(x)$. As a result, the electron effective mass at Γ was found to be isotropic and its value is practically independent of the k-direction for x ranging from 0 to 1. The same trend is shown by the effective mass at X in the X–L direction. The latter mass, however, shows an anisotropic behaviour in the X–Γ direction, which depends on the alloy composition. This anisotropy can be evaluated more accurately using a $\boldsymbol{k}\cdot\boldsymbol{p}$ method.

Table 3. Electron effective masses in units of the free electron mass in zinc-blende GaN and AlN.

Material	Calculated value	Experimental value
GaN	0.127[a]; 0.11[b]; 0.13[c] 0.15[d]; 0.15[e]	0.15[f]
AlN	0.209[a]; 0.19[b];0.21[c] 0.21[d]; 0.25[e]	

[a] Present work.
[b] Reference [17].
[c] Reference [12].
[d] Reference [18].
[e] Reference [3].
[f] Reference [19].

2.3. Calculation of band offsets for strained $Al_{1-x}Ga_xN/Al_{1-y}Ga_yN$ interfaces

Zinc-blende GaN and AlN have lattice constants of 4.37 and 4.5 Å respectively [11]. For a $Al_{1-x}Ga_xN/Al_{1-y}Ga_yN$ heterostructure with the growth direction along $\langle 001 \rangle$, the lattice mismatch gives rise to a biaxial strain in the (001) plane. The effect of this strain on the energy band edges can be decomposed into hydrostatic and uniaxial contributions. The hydrostatic strain shifts the overall energetic positions of the bands. The shear-strain component can split degenerate bands and also leads to an additional splitting of the valence band energies when it is coupled to the spin–orbit interaction. For the Δ conduction band under [001] uniaxial strain, the two valleys along [001] (denoted as Δ_2) and the four along [100] and [010] (denoted as Δ_4) shift with respect to their zero-strain position [20]. However, the Γ conduction band is not affected by this strain component. The strain also influences the band discontinuity at the strained-layer interfaces. To calculate the band offsets for the $Al_{1-x}Ga_xN/Al_{1-y}Ga_yN$ heterointerfaces we adopt the procedure outlined in [7, 20].

The valence and conduction band offsets ΔE_v and ΔE_c are obtained from

$$\Delta E^{str}_{v_{hh,lh}} = E^{str}_{v_{hh,lh}}(Al_{1-x}Ga_xN) - E^{uns}_{v_{hh,lh}}(Al_{1-y}Ga_yN) = \Delta E^{uns}_{v_{hh,lh}} + \delta E^{hy}_{v} + \delta E^{sh}_{v_{hh,lh}} \qquad (5a)$$

and

$$\Delta E^{str}_{c} = E^{str}_{c}(Al_{1-x}Ga_xN) - E^{uns}_{c}(Al_{1-y}Ga_yN) = \Delta E^{uns}_{v} + \Delta E^{uns}_{g} + \delta E^{sh}_{c} + \delta E^{hy}_{c} \qquad (5b)$$

where ΔE^{uns}_{v} is the natural valence band discontinuity and ΔE^{uns}_{g} is the band-gap difference. $\delta E^{hy}_{v,c}$ and $\delta E^{sh}_{v,c}$ are the band energy shifts under hydrostatic and uniaxial stains for the valence and conduction bands respectively. The subscripts *hh* and *lh* stand for heavy hole and light hole respectively.

Using the above set of equations, we have calculated the valence band and the conduction band offsets for lattice-matched and pseudomorphically strained $Al_{1-x}Ga_xN/Al_{1-y}Ga_yN$ heterostructures as a function of x and y over the whole range of compositions. The parameters used in the calculation are taken from [11, 12, 17, 21–23] and listed in table 4. For $Al_{1-x}Ga_xN$ alloys, linear interpolation tends to be a good approximation in evaluating these parameters. Values of the average valence band energies $E_{v,av}$ [7, 20] for AlN and GaN are not available. Van de Walle and Neugebauer [23] have calculated a natural valence band line-up for the (110) AlN/GaN interface using an *ab initio* pseudopotential approach; the band discontinuity is of the order of 0.7 eV. They also carried out calculations of the valence band line-up for an oriented (001) AlN/GaN interface. They found that the band offset for this interface agrees with the results obtained for (110) to within 0.1 eV. On the other hand, using an *ab initio* all-electron band-structure method, Wei and Zunger [22] calculated the natural band offset ΔE_v between III–V semiconductor compounds. The relevant value for the valence band offset at the AlN/GaN heterointerface is 0.8 eV. In the following, we will adopt the common value 0.8 eV as a parameter in our calculations. Conduction band offsets ΔE^{uns}_{c} were deduced

Table 4. Parameters used for the band-offset calculations. All symbols have their conventional meanings as given in their respective references.

	a (Å)	c_{11} (GPA)	c_{12} (GPA)	Δ_0 (eV)	E_v^{uns} (eV)	a_v (eV)	b (eV)	a_c (eV)	Ξ_u^{Δ} (eV)
AlN	4.37[a]	304[b]	160[b]	0.011[c]	−1.52[d]	2.3[e]	−1.5[e]	−6.8[e]	6.6[f]
GaN	4.5[a]	293[b]	159[b]	0.011[c]	−0.72[d]	2.0[e]	−1.7[e]	−6[e]	7.1[f]

[a] Reference [11].
[b] Reference [21].
[c] Reference [17].
[d] Reference [22].
[e] Reference [23].
[f] Reference [12].

from our calculated band gaps. The results are depicted in figure 3. In the composition range $0 \leqslant x \leqslant 0.43$, the conduction band minima of $Al_{1-x}Ga_xN$ are at Δ and therefore are subject to hydrostatic and shear shifts. In addition, under uniaxial strain, the Δ_2 and the Δ_4 bands shift in opposite directions with respect to the unstrained Δ position. In figure 3(a) we plotted only the band offsets corresponding to the lowest conduction bands. For $0.43 \leqslant x \leqslant 1$, the conduction band minimum of the $Al_{1-x}Ga_xN$ alloy is at Γ and so is not affected by the shear strain. The calculated valence band offsets (VBOs) $\Delta E_{v,hh}^{str}$ and $\Delta E_{v,lh}^{str}$ for the (001)-oriented $Al_{1-x}Ga_xN/Al_{1-y}Ga_yN$ interfaces are depicted in figure 3(b). As seen in figure 3, it is found that:

(i) for strained $Al_{1-x}Ga_xN$/AlN heterointerfaces, the line-up is of 'type I', meaning that the band gap of the overlayer $Al_{1-x}Ga_xN$ falls completely inside the band gap of AlN;
(ii) considering $Al_{1-y}Ga_yN$ as a substrate, the band alignment is (separately) of 'type I' in the strained $Al_{1-x}Ga_xN$ for $x < y$ and in the relaxed $Al_{1-y}Ga_yN$ for $x > y$;
(iii) for $Al_{1-x}Ga_xN$/GaN interfaces, the line-up is of 'type I' in GaN, which means that the band gap of the relaxed GaN falls completely inside the band gap of the $Al_{1-x}Ga_xN$ strained layer;
(iv) the valence band discontinuity shows a nearly linear variation versus x with an average slope of 0.84 and a bowing parameter of 0.023 for $0 \leqslant y \leqslant 1$.

As reported in a recent review paper by Vurgaftman *et al* [3], there have been experimental attempts to evaluate the VBO at both zinc-blende and wurtzite GaN/AlN interfaces. Sitar *et al* [24] have obtained a VBO of 1.4 eV from fits to optical measurements on cubic GaN/AlN superlattices. Baur *et al* [25], however, found a valence band discontinuity of 0.5 eV by measuring the difference between the energy levels of an acceptor ion in the two materials. X-ray photoemission spectroscopy yielded a VBO of 0.7 eV for wurtzite GaN/AlN [26]. Using the same experimental procedure, Waldrop and Grant [27] have obtained a different value of 1.36 eV. Those authors also reported a nearly linear VBO variation for $Al_{1-x}Ga_xN$ with a positive bowing parameter of 0.59 eV [28]. With the use of x-ray and ultraviolet photoelectron spectroscopy, King *et al* [29] found that the GaN/AlN VBO ranges from 0.5 to 0.8 eV, depending on the growth temperature. They claimed that the differences in VBO arise from strain, defects and film stoichiometry effects. Theoretically, *ab initio* calculations of the valence band discontinuity were performed for both zinc-blende and wurtzite AlN/GaN interfaces [3]. The VBOs obtained range from 0.7 to 0.85 eV. Using an empirical tight-binding calculation, Monch [30] has obtained a lower value of 0.6 eV. Our result for the VBO at AlN/GaN interface is of the order of 0.82 eV. It agrees well with the calculated values and is close to the average of the measured ones. Unlike in the valence band case, there are no reports of conduction band discontinuity. Due to the lack of band-offset data for $Al_{1-x}Ga_xN$ alloys,

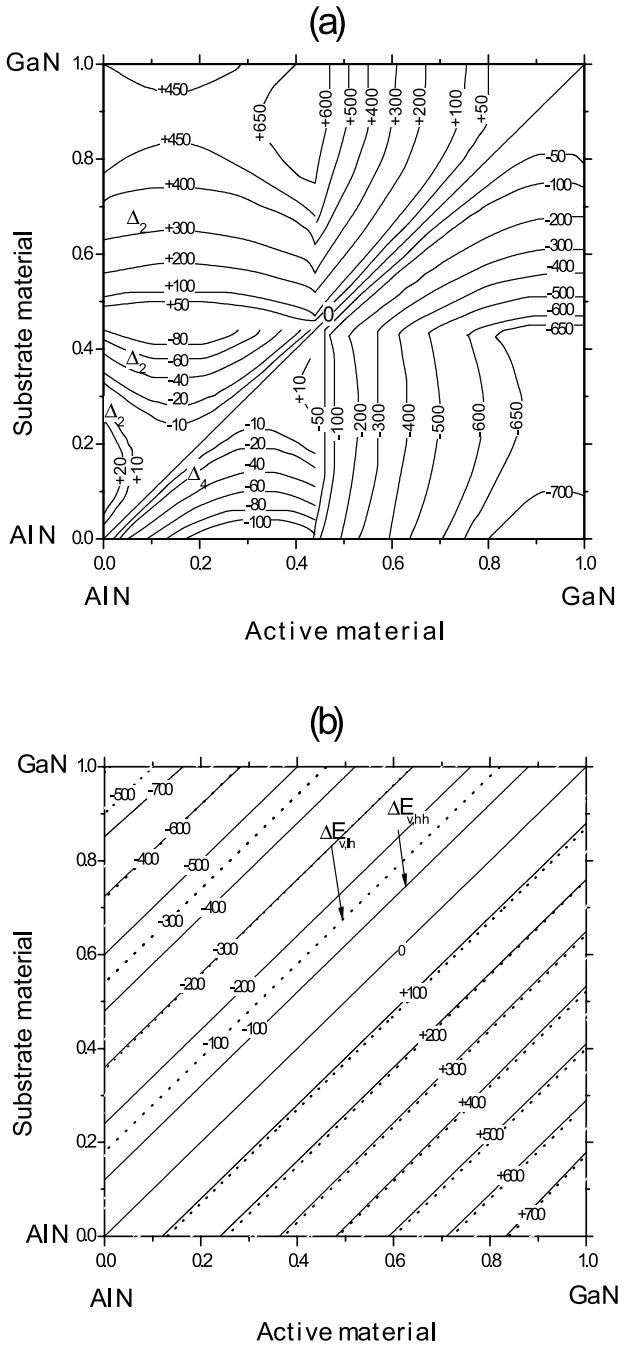

Figure 3. (a) Conduction band offsets $E_c(x) - E_c(y)$ and (b) VBOs $E_v(x) - E_v(y)$ for the heavy holes (solid lines) and light holes (dotted lines) at the $Al_{1-x}Ga_xN/Al_{1-y}Ga_yN$ heterointerfaces. The labels in (a) refer to the conduction band minima in the strained and relaxed materials. All values are expressed in millielectron volts.

our systematical calculations can provide useful information on the compositional dependence of band offsets. They are also of great interest in the design of quantum heterostructure devices using $Al_{1-x}Ga_xN$.

3. Summary

An empirical pseudopotential scheme is used to investigate the electronic properties of zinc-blende $Al_{1-x}Ga_xN$. The results are shown to be in agreement with existing data. The effect of the compositional disorder has been studied and is found to be relatively weak. Based on a model solid theory, estimates of valence and conduction band offsets for lattice-matched and pseudomorphically strained $Al_{1-x}Ga_xN/Al_{1-y}Ga_yN$ heterostructures are presented. In view of the dispersion in the outcome of experiments and the lack of theoretical calculations, our results seem likely to be useful as a reference and more especially in the design of $Al_{1-x}Ga_xN$ structures for wide-gap device applications.

Acknowledgments

One of us (NB) would like to thank the Faculty of Science of Monastir, Monastir, Tunisia, in particular the UR of Solid State Physics, for financial support and kind hospitality extended during his stay at Monastir. Part of this work was done at the International Centre for Theoretical Physics (ICTP), Trieste, Italy. NB and MS gratefully acknowledge the ICTP support received during their stay at the Centre.

References

[1] Razeghi M and Rogalski A 1996 *J. Appl. Phys.* **79** 7433
[2] Jain S C, Willander M, Narayan J and Van Overstraeten R 2000 *J. Appl. Phys.* **87** 965
[3] Vurgaftman I, Meyer J R and Ram-Mohan L R 2001 *J. Appl. Phys.* **89** 5815 and references therein
[4] Shan W, Ager J W III, Yu K M, Walukiewicz W, Haller E E, Martin M C, McKinney W R and Yang W 1999 *J. Appl. Phys.* **85** 8505
[5] Rodrigues S C P, Rosa A L, Scolfaro L M R, Beliaev D, Leite J R, Enderlein R and Alves J L A 1998 *Semicond. Sci. Technol.* **13** 981
[6] Albanesi E A, Lambrecht W R L and Segall B 1993 *Phys. Rev.* B **48** 17 841
[7] Van de Walle C G and Martin R 1986 *Phys. Rev.* B **34** 5621
Van de Walle C G 1989 *Phys. Rev.* B **39** 1871
[8] Kobayasi T and Nara H 1993 *Bull. Coll. Med. Sci., Tohoku Univ.* **2** 7
[9] Lee S J, Kwon T S, Nahm K and Kim C K 1990 *J. Phys.: Condens. Matter* **2** 3253
[10] Bouarissa N 1998 *Phys. Lett.* A **245** 285
[11] Stampfl C and van de Walle C G 1999 *Phys. Rev.* B **59** 5521
[12] Fan W J, Li M F, Chong T C and Xia J B 1996 *J. Appl. Phys.* **79** 188
[13] Christensen N E and Gorczyca I 1994 *Phys. Rev.* B **50** 4397
[14] Brunner D, Angerer H, Bustarret E, Freudenberg F, Heopler R, Dimitrov R, Ambacher O and Stutzmann M 1997 *J. Appl. Phys.* **82** 5090
[15] Huang Tzu-Fang and Harris J S 1998 *Appl. Phys. Lett.* **72** 1158
[16] Kassali K and Bouarissa N 2000 *Solid-State Electron.* **44** 501
[17] Pugh S K, Dugdale D J, Brand S and Abram R A 1999 *Semicond. Sci. Technol.* **14** 23
[18] Meney A T, O'Reilly E P and Adams A R 1996 *Semicond. Sci. Technol.* **11** 897
[19] Fanciulli M, Lei T and Moustakas T D 1993 *Phys. Rev.* B **48** 15 144
[20] Ben Zid F, Bhouri A, Mejri H, Tlili R, Said M, Lazzari J L, Arnaud d'Avitaya F and Derrien J 2002 *J. Appl. Phys.* **91** 9170
[21] Wright A F 1997 *J. Appl. Phys.* **82** 2833
[22] Wei S H and Zunger A 1998 *Appl. Phys. Lett.* **72** 2011
[23] Van de Walle C G and Neugebauer J 1997 *Appl. Phys. Lett.* **70** 2577

[24] Sitar Z, Paisley M J, Ruan J, Choyke J W and Davis R F 1992 *J. Mater. Sci. Lett.* **11** 261
[25] Baur J, Maier K, Kunzer M, Kaufmann U and Schneider J 1994 *Appl. Phys. Lett.* **65** 2211
[26] Martin G A, Botchkarev A, Rockett A and Morkoc H 1996 *Appl. Phys. Lett.* **68** 2541
[27] Waldrop J R and Grant R W 1996 *Appl. Phys. Lett.* **68** 2879
[28] Beach R A, Piquette E C, Grant R W and McGill T C 1998 *MRS Symp. Proc.* **482** 775
[29] King S W, Ronning C, Davis R F, Benjamin M C and Nemanich R J 1998 *J. Appl. Phys.* **84** 2086
[30] Monch W 1996 *J. Appl. Phys.* **80** 5076